Figure S1

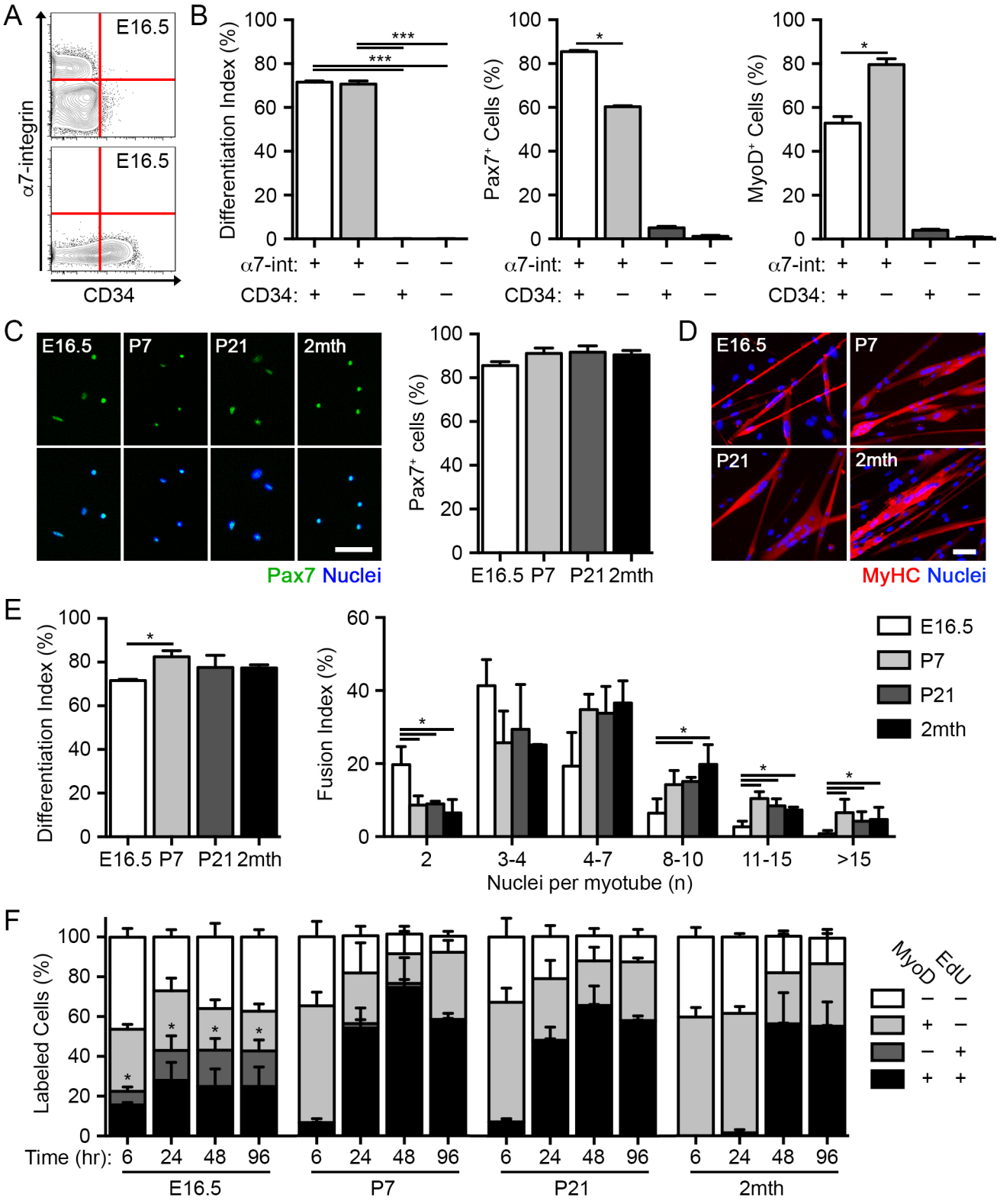
A
E16.5
E16.5
α7-integrin
CD34
B
Differentiation Index (%)
***
***
α7-int: + + – –
CD34: + – + –
Pax7⁺ Cells (%)
*
α7-int: + + – –
CD34: + – + –
MyoD⁺ Cells (%)
*
α7-int: + + – –
CD34: + – + –
C
E16.5
P7
P21
2mth
Pax7 Nuclei
Pax7⁺ cells (%)
E16.5 P7 P21 2mth
D
E16.5
P7
P21
2mth
MyHC Nuclei
E
Differentiation Index (%)
E16.5 P7 P21 2mth
Fusion Index (%)
E16.5
P7
P21
2mth
2
3-4
4-7
8-10
11-15
>15
Nuclei per myotube (n)
F
Labeled Cells (%)
Time (hr): 6 24 48 96 6 24 48 96 6 24 48 96 6 24 48 96
E16.5
P7
P21
2mth
MyoD EdU
– –
+ –
– +
+ +

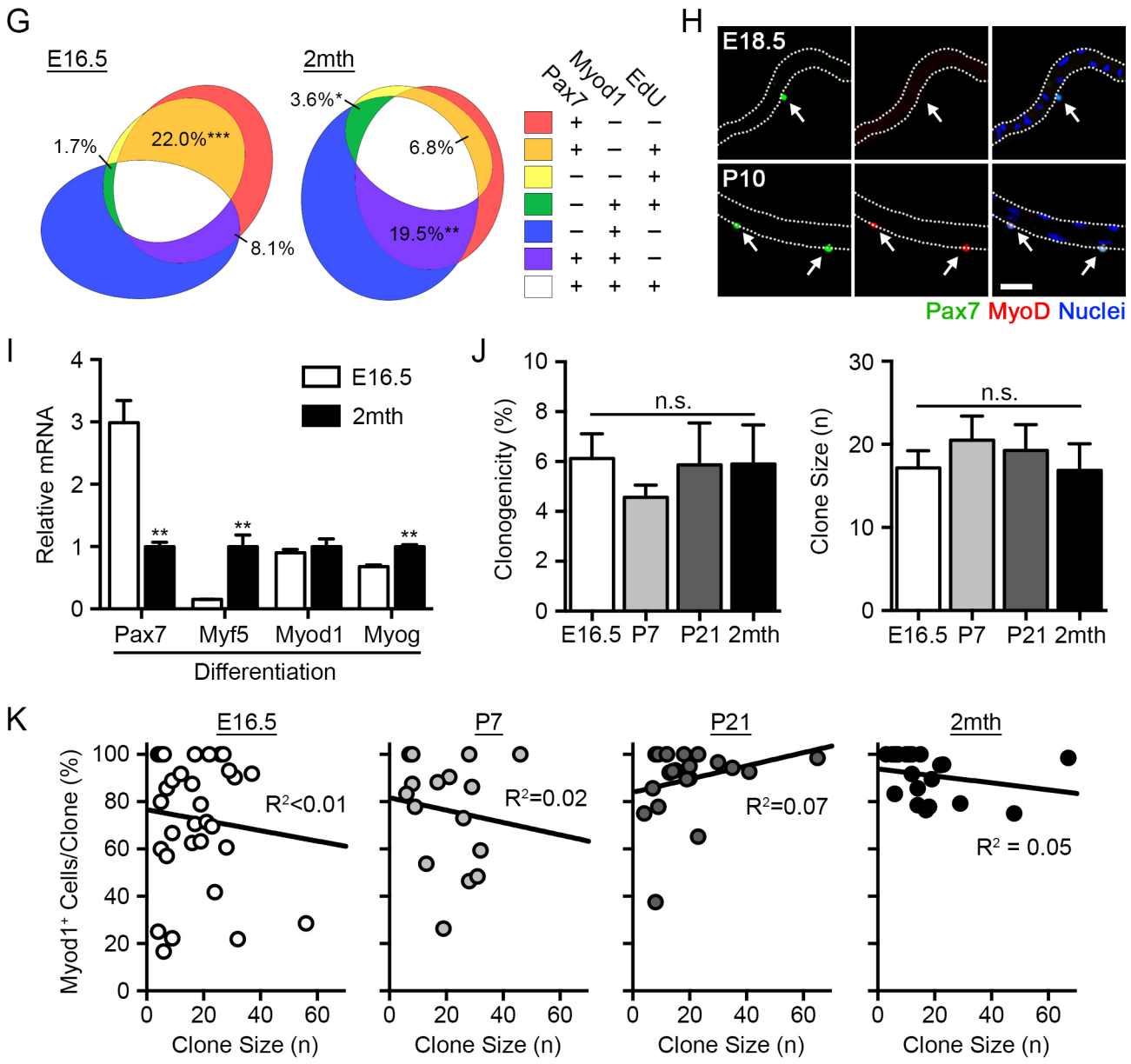

Figure S1, related to Figure 1. Isolation and characterization of fetal MuSC.

(**A**) Fluorescence minus one (FMO) controls to determine gating strategies for FACS-based cell isolation of fetal muscle cells at embryonic day 16.5 (E16.5) gated for α7-integrin and CD34.

(**B**) Quantification of differentiation index of myosin heavy chain (MyHC)-expressing myotubes from the four fractions of freshly isolated fetal (E16.5) muscle cells based on α7-integrin CD34 expression after 3 d in differentiation conditions (left, n = 3-5). Quantification of the percentage of $Pax7^+$ and $Myod1^+$ cells

from the four fractions of freshly isolated fetal (E16.5) muscle cells based on α7-integrin CD34 expression after six hours in culture (right, n = 3-5).

(**C**) Representative images of freshly isolated, Pax7-expressing MuSC at the indicated developmental stages after 6 hours in culture (green = Pax7, blue = nuclei). Scale bar, 50 μm (left). Quantification of the percentage of $Pax7^+$ cells (right, n = 3-5).

(**D**) Representative images of myosin heavy chain (MyHC)-expressing myotubes after 3 d in differentiation conditions. Scale bar, 50 μm.

(**E**) Quantification of differentiation index (left) and fusion index in myosin heavy chain (MyHC)-expressing myotubes after 3 d in differentiation conditions (right, n = 3-5).

(**F**) Quantification of the percentage of MyoD expression and EdU incorporation in freshly isolated MuSC from the four developmental stages cultured for 4 d under growth conditions (n = 3-6).

(**G**) Venn diagram of Pax7 and MyoD expression and EdU incorporation in freshly isolated fetal (E16.5) and adult (2 mth) MuSC cultured for 4 d under growth conditions (n = 3) (Micallef and Rodgers, 2014).

(**H**) Representative images of freshly isolated single myofibers from embryonic day 18.5 (E18.5) and postnatal day 10 (P10) hind limb muscle (green = Pax7, red = Myod1, blue = nuclei). Scale bar, 20 μm.

(**I**) Pax7, Myf5, Myod1 and Myog mRNA levels in fetal (E16.5) and adult (2 mth) MuSC in differentiation conditions (n = 3-5).

(**J**) Quantification of clonogenicity (left) and clone size (right) of MuSC at the indicated developmental stages after 5 d in culture (n = 3-4).

(**K**) Quantification of the correlation between the percentage of $Myod1^+$ cells within individual clones and clone size of MuSC at the indicated developmental stages after 5 d in culture (n = 15-33 clones).

Data are represented as average ± SEM. Student's t test was used for all statistical analyses (***P < 0.001, **P < 0.01, *P < 0.05). Linear regression analyses presented with coefficient of determination for goodness of fit measures.

Figure S2

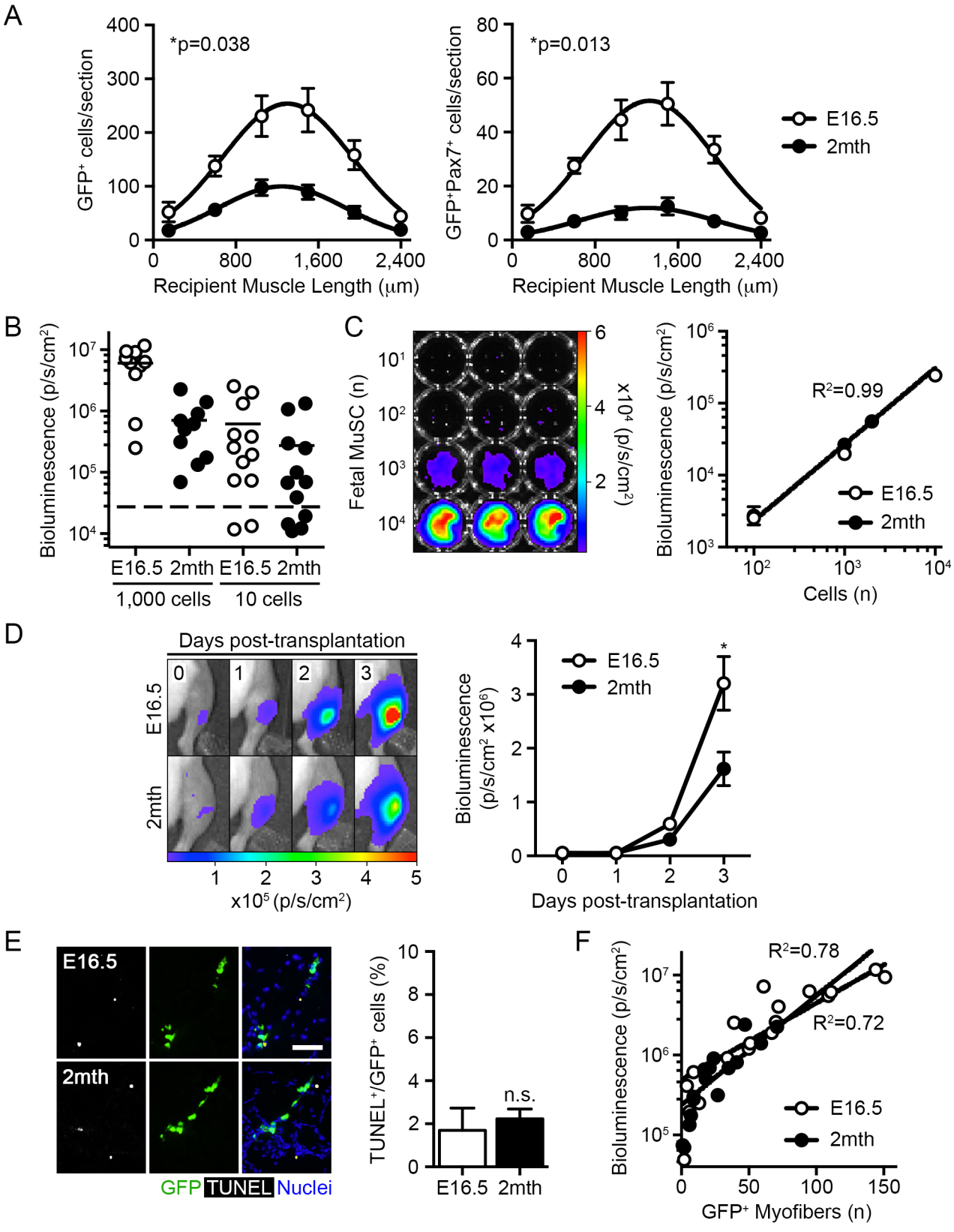

Figure S2, related to Figure 2. Fetal MuSC robustly contribute to muscle repair.

(**A**) Quantification of the number of GFP^+ and GFP^+Pax7^+ donor MuSC at 3 d post-transplantation (n = 6).

(**B**) Quantification of bioluminescence (BLI) emission in individual recipient mice following 1,000 or 10 fetal (E16.5) and adult (2 mth) MuSC transplantation at 25 d (n = 10-12).

(**C**) Representative BLI image of fetal MuSC plated in a 96-well plate and imaged immediately after plating (values indicated as photons s^{-1} cm^{-2}, left). Quantification of the correlation between BLI signaling and the number of MuSC plated (10-10,000 cells) (n = 3, right).

(**D**) Representative BLI images in recipient mice at the indicated time points post-transplantation of 5,000 MuSC (values indicated as photons s^{-1} cm^{-2}, left). Quantification of BLI emission following 5,000 MuSC transplantation over 3 d (n = 8-11, right).

(**E**) Representative images of $TUNEL^+GFP^+$ donor MuSC at 1 d post-transplantation (left). Quantification of the percentage of $TUNEL^+$ donor MuSC at 1 d post-transplantation (n = 4, right).

(**F**) Quantification of the correlation between BLI emission and the number of GFP^+ donor myofibers in individual transplants at 25 d post-transplantation (n = 10-12).

Data are represented as average ± SEM. Student's t test was used for all statistical analyses (*P < 0.05). Linear regression analyses presented with coefficient of determination for goodness of fit measures.

Figure S3

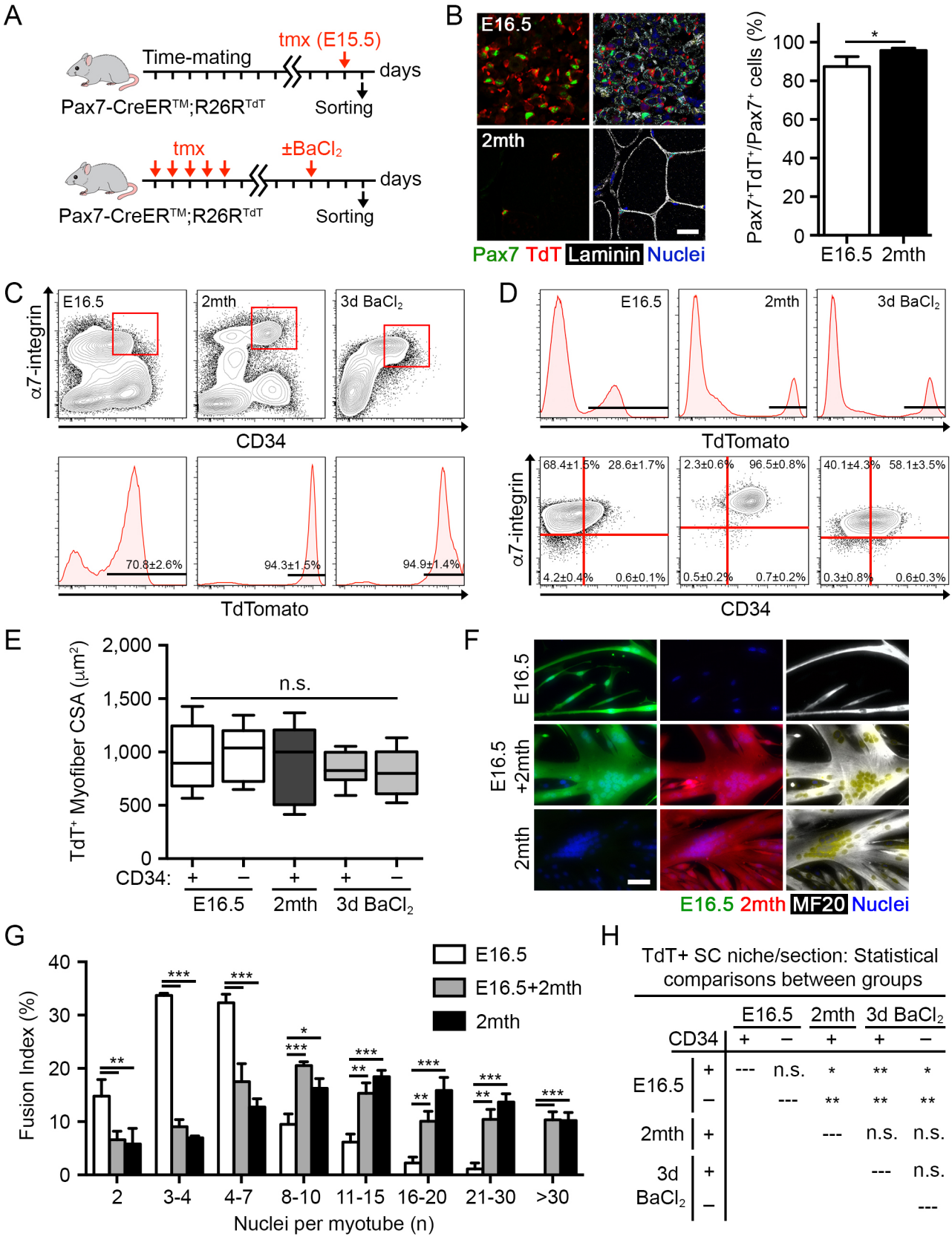

		E16.5		2mth	3d $BaCl_2$	
CD34		+	–	+	+	–
E16.5	+	---	n.s.	*	**	*
	–		---	**	**	**
2mth	+			---	n.s.	n.s.
3d $BaCl_2$	+				---	n.s.
	–					---

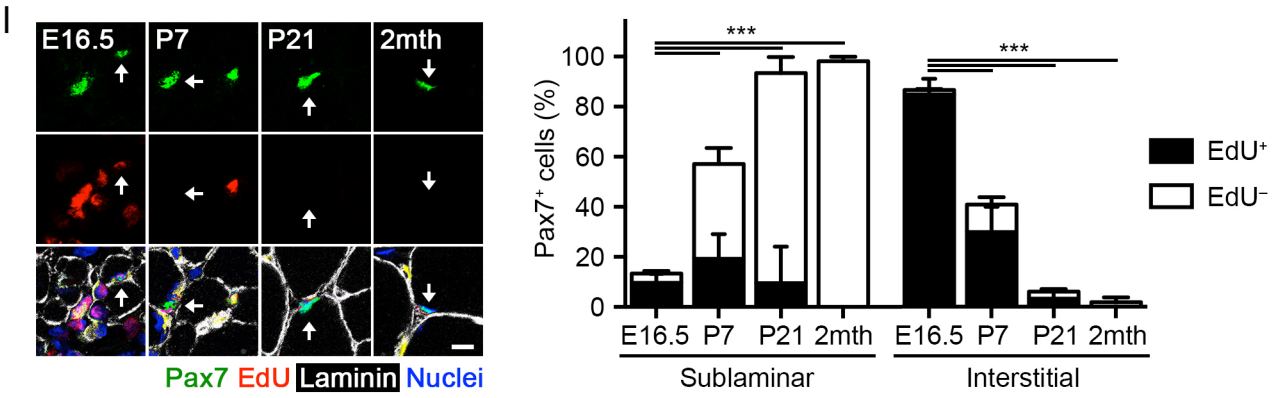

Figure S3, related to Figure 3. Labeling, isolation and characterization of Pax7^{+} fetal and adult MuSC from Pax7-CreER^{TM};R26R^{TdT} mice.

(**A**) Schematic representation of tamoxifen (tmx) treatment of Pax7-CreER^{TM};R26R^{TdT} mice at fetal and adult stages.

(**B**) Representative images of fetal (E16.5) hind limb muscle and adult (2 mth) tibialis anterior muscle in Pax7-CreER^{TM};R26R^{TdT} mice following tmx treatment (green = Pax7, red = TdTomato, white = laminin, blue = nuclei). Scale bar, 50 μm (left). Quantification of the efficiency of recombination via TdTomato expression in Pax7-CreER^{TM};R26R^{TdT} fetal and adult muscles (right).

(**C**) Flow cytometry analysis and quantification of TdTomato expression in fetal (E16.5), adult (2 mth) and adult activated (2 mth, 3 d post-barium chloride injury) Pax7-CreER^{TM};R26R^{TdT} MuSC after gating for α7-integrin and CD34 (n = 3-5).

(**D**) Flow cytometry analysis and quantification of α7-integrin and CD34 expression in fetal (E16.5), adult (2 mth) and adult activated (2 mth, 3 d post-barium chloride injury) Pax7-CreER^{TM};R26R^{TdT} MuSC after gating for TdTomato expression (n = 3-5).

(**E**) Quantification of myofiber cross-sectional area in donor-derived TdTomato^{+} myofibers 15 d post-transplantation (n = 6).

(**F**) Representative images of myosin heavy chain (MyHC)-expressing myotubes from GFP^{+} fetal (E16.5) and TdTomato^{+} adult (2 mth) Pax7-CreER^{TM};R26R^{TdT} MuSC either alone in or in co-culture after 3 d in differentiation conditions. Scale bar, 50 μm.

(**G**) Quantification of fusion index in myosin heavy chain (MyHC)-expressing myotubes either alone in or in co-culture after 3 d in differentiation conditions (n = 3).

(**H**) Matrix describing the statistical significance between groups when measuring satellite cell niche engraftment 15 d post-transplantation (n = 6).

(**I**) Representative images of $Pax7^+$ expression and EdU incorporation in fetal (E16.5), postnatal day 7 and 21 (P7, P21) and adult (2 mth) hind limb muscles (green = Pax7, red = EdU, white = laminin, blue = nuclei). Scale bar, 50 μm. Arrows indicate $Pax7^+$ cells positioned in the satellite cell niche (left). Quantification of the percentage of $Pax7^+EdU^+$ cells in sublaminar or interstitial position at each developmental time point (n = 3-5, right).

Data are represented as average ± SEM. Student's t test was used for all statistical analyses (***P < 0.001, **P < 0.01, *P < 0.05) except (**E**), where one-way ANOVA with Tukey's post-hoc test was used and (**G**), where two-way ANOVA with Tukey's post-hoc test was used.

Figure S4

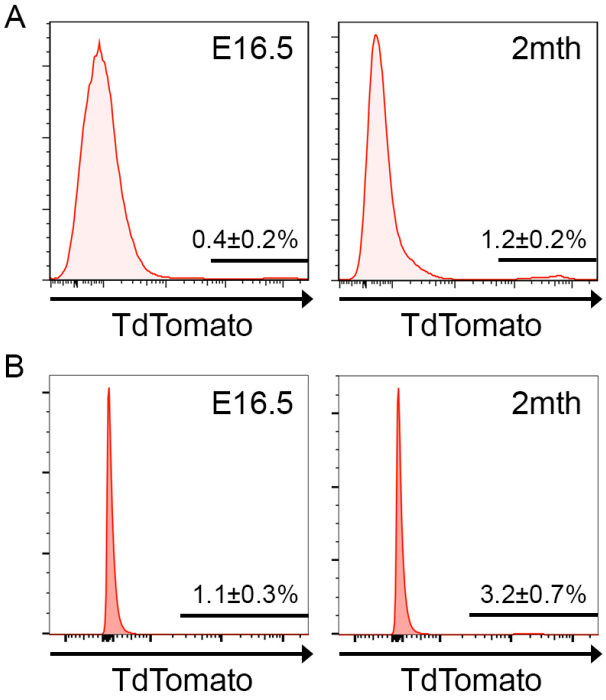

Figure S4, related to Figure 4. Serial transplantation of Pax7^{+} fetal and adult MuSC from Pax7-CreER^{TM};R26R^{TdT} mice.

(**A**) Fluorescent-based cell sorting (FACS) of engrafted fetal (E16.5) and adult (2 mth) MuSC at 21 d post-transplantation (n = 8).

(**B**) Fluorescent-based cell sorting (FACS) of engrafted fetal (E16.5) and adult (2 mth) MuSC at 24 d post-transplantation and 3 d post-barium chloride injury (n = 4).

Figure S5

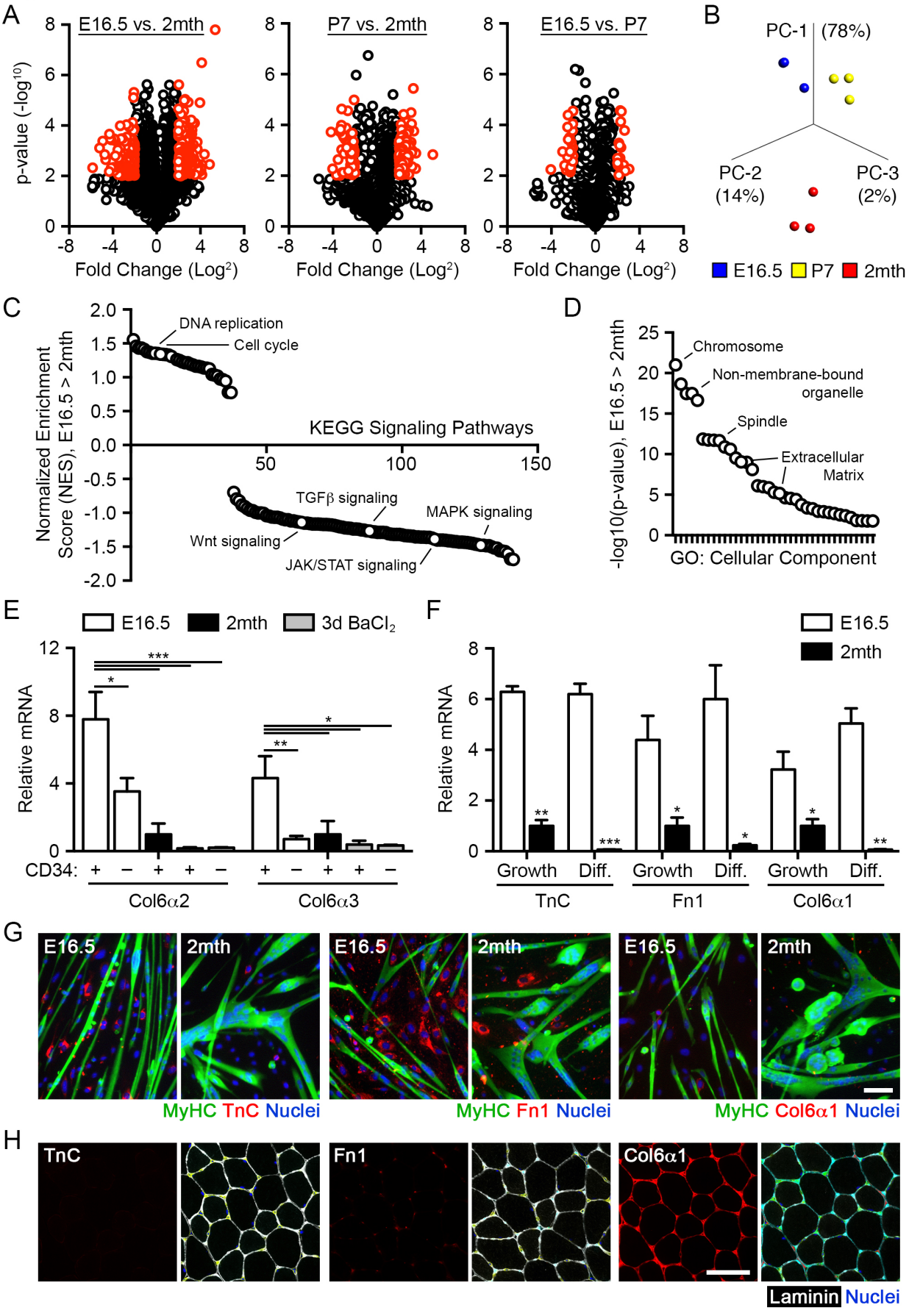
A
E16.5 vs. 2mth
P7 vs. 2mth
E16.5 vs. P7
p-value (-log10)
Fold Change (Log2)
B
PC-1 (78%)
PC-2 (14%)
PC-3 (2%)
E16.5 P7 2mth
C
Normalized Enrichment Score (NES), E16.5 > 2mth
DNA replication
Cell cycle
KEGG Signaling Pathways
TGFβ signaling
MAPK signaling
Wnt signaling
JAK/STAT signaling
D
-log10(p-value), E16.5 > 2mth
Chromosome
Non-membrane-bound organelle
Spindle
Extracellular Matrix
GO: Cellular Component
E
E16.5 2mth 3d BaCl2
Relative mRNA
CD34:
Col6α2
Col6α3
F
E16.5
2mth
Relative mRNA
Growth Diff.
TnC
Fn1
Col6α1
G
E16.5
2mth
MyHC TnC Nuclei
MyHC Fn1 Nuclei
MyHC Col6α1 Nuclei
H
TnC
Fn1
Col6α1
Laminin Nuclei

Figure S5, related to Figure 5. Comparative gene expression profiling of freshly isolated fetal, neonatal and adult MuSC.

(**A**) Volcano plots of microarray analyses of freshly isolated fetal (E16.5), postnatal day 7 (P7) and adult (2mth) MuSC. Probes with a p-value of $-\log^{10} > 2$ and fold change of $\log^2 > 2$ in red.

(**B**) Principle component analysis of microarray results of fetal (E16.5), postnatal day 7 (P7) and adult (2 mth) MuSC. Each principal component is ordered according to the magnitude of its eigenvalue, represented as a percentage.

(**C**) Gene set enrichment analysis (GSEA) in fetal (E16.5) and adult (2 mth) MuSC based on KEGG signaling pathway enrichment and ranked on the basis of their normalized enrichment score (NES).

(**D**) Gene set enrichment analysis (GSEA) in fetal (E16.5) and adult (2 mth) MuSC based on the gene ontology (G) cellular component gene set. Scores used to rank genes were calculated as $-\log_{10}$(p-value).

(**E**) Quantification of Col6α2 and Col6α3 mRNA levels from freshly isolated fetal (E16.5), adult (2 mth) and adult activated (2 mth, 3 d barium chloride injury) MuSC from Pax7-CreER^{TM};R26R^{TdT} mice (n = 3-6).

(**F**) TnC, Fn1 and Col6α1 mRNA levels in fetal (E16.5) and adult (2 mth) MuSC cultured in growth and differentiation conditions (n = 3).

(**G**) Representative images of fetal (E16.5) and adult (2 mth) myosin heavy chain (MyHC)-expressing myotubes after 3 d in differentiation conditions (green = MF20, red = TnC, Fn1 or Col6α1 as labeled, blue = nuclei). Scale bar, 50 μm.

(**H**) Representative images of the adult (2 mth) tibialis anterior muscle (red = TnC, Fn1 or Col6α1 as labeled, white = laminin, blue = nuclei). Scale bar, 200 μm.

Data are represented as average ± SEM. Student's t test was used for all statistical analyses (***P < 0.001, **P < 0.01, *P < 0.05) except (**E**), where one-way ANOVA with Tukey's post-hoc test was used.

Figure S6

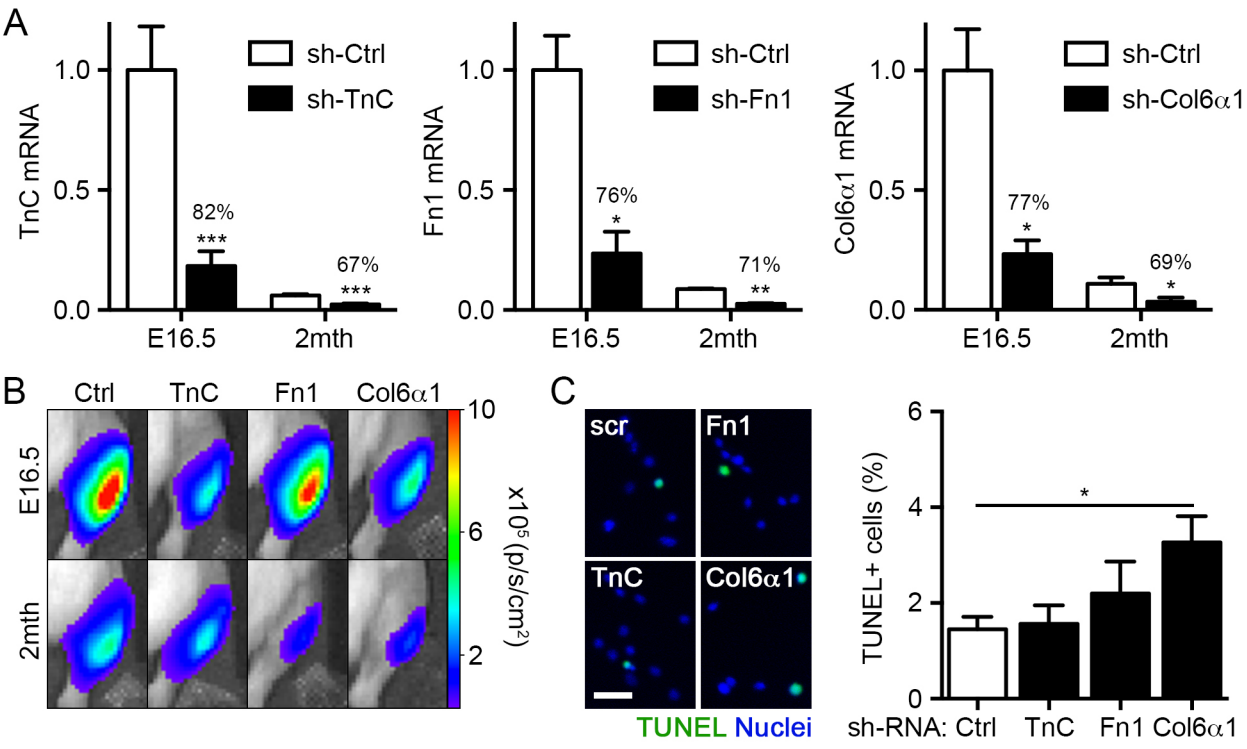

Figure S6, related to Figure 6. Stage-specific role of ECM proteins in regulating MuSC regenerative potential.

(**A**) TnC, Fn1 and Col6α1 mRNA levels in fetal (E16.5) and adult (2 mth) MuSC treated with sh-TnC, sh-Fn1, sh-Col6α1 or sh-control lentiviruses and cultured for 3 d post-infection (n = 3-8). The percentage knockdown for each shRNA is stated for each comparison.

(**B**) Representative images of bioluminescence (BLI) emission in recipient mice receiving fetal (E16.5) and adult (2 mth) MuSC treated with sh-TnC, sh-Fn1, sh-Col6α1 or sh-control lentiviruses 15 d post-transplantation (values are indicated as photons s^{-1} cm^{-2}).

(**C**) Representative images of TUNEL performed in fetal (E16.5) MuSC treated with sh-TnC, sh-Fn1, sh-Col6α1 or sh-control lentiviruses and cultured in growth media for 3 d (green = TUNEL, blue = nuclei). Scale bar, 50 μm (left). Quantification of the percentage of apoptotic $TUNEL^+$ nuclei (n = 3, right).

Data are represented as average ± SEM. Student's t test was used for all statistical analyses (***P < 0.001, **P < 0.01, *P < 0.05) except (**C**), where one-way ANOVA with Tukey's post-hoc test was used.

Figure S7

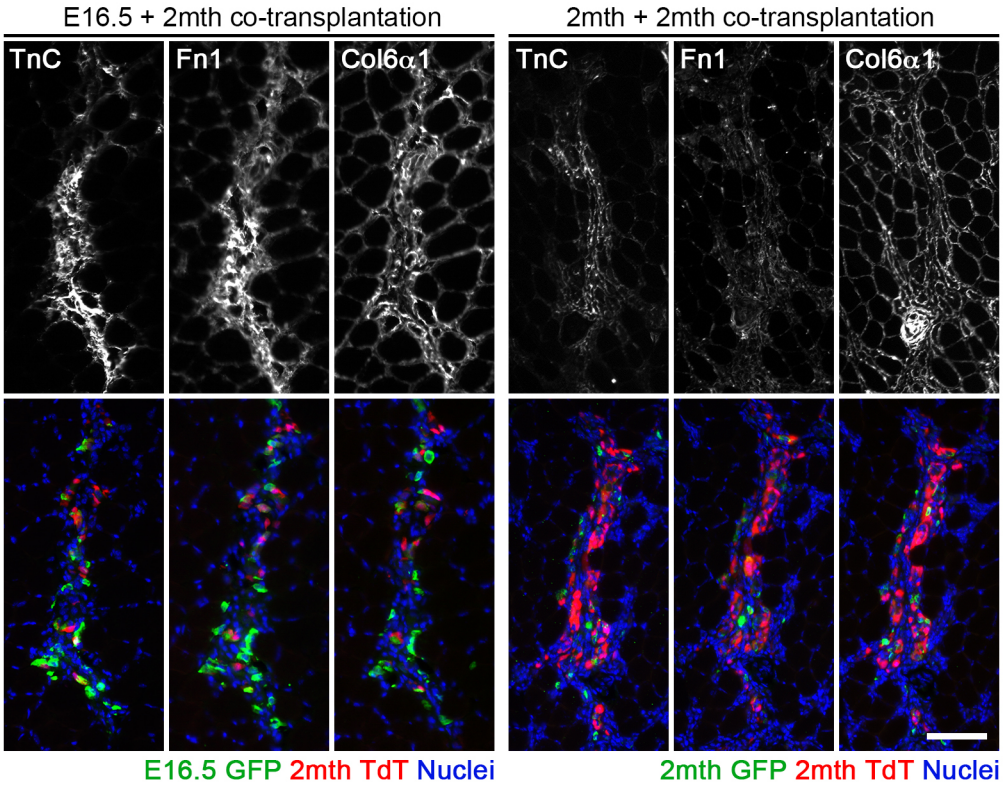

Figure S7, related to Figure 7. Co-transplantation of fetal MuSC and adult MuSC during muscle repair.

Representative images of TnC, Fn1 and Col6α1 expression and donor-derived GFP^+ fetal (E16.5) and $TdTomato^+$ adult (2 mth) MuSC 3 d post-transplantation (green = GFP, red = TdTomato, white = TnC, Fn1 or Col6α1 as labeled, blue = nuclei). Scale bar, 50 μm.

Movie S1, related to Figure 1. Time-lapse recording of the fetal (E16.5) MuSC cell division represented in Figure 1, maintained in growth media from 35 – 45 h post-plating.

Movie S2, related to Figure 1. Time-lapse recording of the adult (2 mth) MuSC cell division represented in Figure 1, maintained in growth media from 35 – 45 h post-plating.

Table S1, related to Figure 5. Pathway analysis from microarray analyses. Gene network generation and pathway analysis of genes differentially expressed specifically in fetal MuSC (filtered against both neonatal and adult MuSC), performed with Ingenuity Pathway Analysis (Qiagen). Analysis consists of molecular networks, canonical pathways, upstream regulators and differentially expressed molecules. Includes direct and indirect relationships. Filtering cutoffs were chosen as p-value < 0.01 and log ratio > 1.0.

Table S2, related to Figure 5. Gene set enrichment analysis and functional annotation from microarray analyses. Statistically significant gene sets derived from KEGG pathway database (http://genome.jp/kegg/pathway.html) comparing fetal (E16.5) and adult (2 mth) MuSC using gene set enrichment analysis (GSEA). Differentially expressed genes comparing fetal (E16.5) and adult (2 mth) MuSC listed in rank order from selected KEGG pathways (MAPK, JAK/STAT, TGFβ, WNT). Differentially expressed genes comparing fetal (E16.5) to either neonatal (P7) or adult (2 mth) MuSC from selected extracellular matrix genes (ECM). Functional annotation of cellular component gene ontology (GO) upregulated in fetal (E16.5) compared to adult (2 mth) MuSC with DAVID Bioinformatics Resources 6.7 (http://david.abcc.ncifcrf.gov).

Table S3, related to Figure 5. Extracellular matrix genes from microarray analyses.

			Fold change		
Symbol	**Gene**	**Identifier**	**E16.5**	**P7**	**2mth**
TnC	Tenascin-C	ILMN_2463181	15.71	6.69	1.00
Gpc3	Glypican 3	ILMN_2719973	9.97	8.53	1.00
Vcan	Versican	ILMN_1247540	7.20	2.56	1.00
Fbln1	Fibulin 1	ILMN_2449644	4.49	2.57	1.00
Lamb1	Laminin, beta 1	ILMN_1253659	3.79	2.80	1.00
Fn1	Fibronectin 1	ILMN_2595714	3.50	1.63	1.00
Col18a1	Collagen, type XVIII, alpha 1	ILMN_2735184	3.45	1.47	1.00
Lum	Lumican	ILMN_3001540	3.27	1.32	1.00
Col8a1	Collagen, type VIII, alpha 1	ILMN_2503553	2.79	0.36	1.00
Col12a1	Collagen, type XII, alpha 1	ILMN_2862538	2.76	1.66	1.00
Gpc1	Glypican 1	ILMN_2635784	2.34	2.32	1.00
Col6a3	Collagen, type VI, alpha 3	ILMN_1249220	2.28	1.20	1.00
Col4a2	Collagen, type IV, alpha 2	ILMN_2822579	2.13	2.26	1.00
Lama5	Laminin, alpha 5	ILMN_2640248	2.11	1.05	1.00

Table S3, related to Figure 5. Extracellular matrix genes from microarray analyses. List of extracellular matrix genes upregulated in fetal (E16.5) compared to neonatal (P7) and adult (2 mth) MuSC as identified in microarray analyses, expressed as fold change relative to adult (2 mth) MuSC. Differentially expressed genes were selected for p-value < 0.01 and fold change > 2.

Table S4, related to Figure 5. Top differentially regulated genes from microarray analyses.

Symbol	Gene	Identifier	Log Ratio	p-value
Dlk1	Delta-like homolog 1	ILMN_1244618	5.351	1.58E-08
Igf2bp3	Insulin-like growth factor 2 binding protein 3	ILMN_1218913	4.856	3.43E-03
H19	H19	ILMN_2906728	4.376	1.38E-03
Xist	X-inactive specific transcript	ILMN_2475156	4.153	8.97E-03
Tsga14	Testis-specific gene A14	ILMN_1228822	4.140	3.56E-03
Tsga14	Testis-specific gene A14	ILMN_2551744	4.122	3.24E-07
Igf2bp3	Insulin-like growth factor 2 binding protein 3	ILMN_1226175	4.077	6.15E-03
Igf2bp1	Insulin-like growth factor 2 binding protein 1	ILMN_3006804	4.074	4.89E-03
Tnc	Tenascin C	ILMN_2463181	3.974	1.23E-05
Tnc	Tenascin C	ILMN_2463180	3.869	7.02E-03
Xist	X-inactive specific transcript	ILMN_1224091	3.857	6.15E-03
Ptn	Pleiotrophin	ILMN_2638114	3.836	3.75E-03
Stab1	Stabilin 1	ILMN_2544343	3.759	5.22E-03
Zcchc5	Zinc finger, CCHC domain containing 5	ILMN_2441346	3.734	5.70E-03
Bex4	Brain expressed, X-linked 4	ILMN_3118584	3.720	5.37E-03
Hist1h2ag	Histone cluster 1, H2ag	ILMN_2981801	3.719	4.45E-04
Kcne1l	Potassium channel, voltage gated subfamily E regulatory beta subunit 5	ILMN_2765662	3.715	8.43E-04
Hist2h2ab	Histone cluster 2, H2ab	ILMN_2785454	3.649	3.13E-03
Tk1	Thymidine kinase 1	ILMN_2605890	3.540	8.83E-03
Nt5dc2	5'-Nucleotidase domain containing 2	ILMN_2660519	3.530	2.70E-03
AW551984	Expressed sequence AW551984	ILMN_2721975	3.472	8.05E-05
Tnni2	Troponin 1, type 2	ILMN_2481133	3.402	1.96E-03
Nusap1	Nucleolar and spindle associated protein 1	ILMN_2653765	3.361	5.73E-04
H19	H19	ILMN_1256343	3.334	7.78E-05
Gpc3	Glypican 3	ILMN_2719973	3.318	1.34E-03
Dlk1	Delta-like homolog 1	ILMN_2771738	3.247	1.52E-04
Uhrf1	Ubiquitin-like with PHD and ring finger	ILMN_2517041	3.233	2.18E-04
Cdc2a	Cyclin-dependent kinase 1	ILMN_2657844	3.227	3.12E-03
Hist1h2ah	Histone cluster 1, H2ah	ILMN_1246108	3.213	1.93E-03
Birc5	Baculoviral IAP repeat containing 5	ILMN_2632712	3.205	4.71E-03
Igfbp2	Insulin-like growth factor binding protein 2	ILMN_1236788	3.181	6.94E-04
Mfap2	Microfibrillar-associated protein 2	ILMN_2981542	3.163	6.01E-05
Prss35	Protease serine 35	ILMN_2609897	3.156	1.93E-03
AI448196	Armadillo repeat containing, X-	ILMN_1246006	3.115	4.29E-03

	linked 4			
Tro	Trophinin	ILMN_2510474	3.081	8.04E-03
AW551984	Expressed sequence AW551984	ILMN_2721980	3.069	2.08E-04
Cdca8	Cell division cycle associated 8	ILMN_2543393	3.044	5.39E-04
2810430P21Rik	Protein phosphatase 1, regulatory subunit 9A	ILMN_2421822	3.006	3.26E-03
Spag5	Sperm associated antigen 5	ILMN_2744217	3.003	2.65E-03
Hist1h2an	Histone cluster 1, H2an	ILMN_1248830	2.972	7.45E-04
Lig1	Ligase 1	ILMN_2595519	2.958	1.20E-04
Hist1h2ad	Histone cluster 1, H2ad	ILMN_2795040	2.951	1.19E-03
Ncaph	Non-SMC condensin 1 complex, subunit H	ILMN_2797642	2.948	1.90E-04
Hist1h2ah	Histone cluster 1, H2ah	ILMN_2730329	2.940	1.76E-03
Tpm2	Tropomyosin 2	ILMN_2482209	2.928	3.67E-04
Epha3	EPH receptor A3	ILMN_2831656	2.927	6.96E-03
Igfbp2	Insulin-like growth factor binding protein 2	ILMN_2930897	2.924	1.48E-03
Ddah1	Dimethylarginine dimethylaminohydrolase 1	ILMN_1256676	2.918	6.59E-04
Tro	Trophinin	ILMN_3129213	2.893	3.35E-03
Mybl2	V-myb avian myeloblastosis	ILMN_2826881	2.890	3.59E-04
Jak1	Janus kinase 1	ILMN_1213278	2.889	1.19E-05
Ptgis	Prostiglandin I2 (prostacyclin) synthase	ILMN_2724942	2.884	8.31E-04
Bex4	Brain expressed, X-linked 4	ILMN_3043587	2.875	5.77E-04
Aurkb	Aurora kinase B	ILMN_1239230	2.851	4.95E-04

Table S4, related to Figure 5. Top differentially regulated genes from microarray analyses. List of genes most upregulated in fetal (E16.5) compared to adult (2 mth) MuSC as identified in microarray analyses. Genes expressed as a log ratio and listed with accompanying p-value.

SUPPLEMENTAL EXPERIMENTAL PROCEDURES

Muscle stem cell (MuSC) isolation. Hind limb muscles of mice at the specified time during development were subjected to enzymatic dissociation (0.2% collagenase and 0.02 units ml^{-1} dispase, Sigma) for 45 min, after which non-muscle tissue was gently removed and the muscle was minced under a dissection microscope and followed by another 45 min incubation. The cell suspension was filtered through a 70 μm nylon filter and incubated with the following biotinylated rat antibodies: CD45 (clone 30-F11), CD11b (cat #553309), CD31 (cat #5011513) and Sca1 (clone E13-161.7) (BD Biosciences). Streptavidin beads (Miltenyi) were then added to the cells together with the following antibodies: α7-integrin–phycoerythrin (cat #R2F2, Ablab) and CD34–Alexa647 (clone RAM34, eBioscience). Magnetic depletion of biotin-positive cells was performed before fractionating the ($CD45^{-}CD11b^{-}CD31^{-}Sca1^{-}$) α7-$integrin^{+}CD34^{+}$ population by flow cytometry (BD FACS Aria) and purity check.

Single myofiber isolation. Single myofibers were prepared as previously described (Sacco et al., 2010). Briefly, the gastrocnemius (GAS) and extensor digitorum longus (EDL) muscles from postnatal mice or hind limb muscles from fetal embryos were harvested and enzymatically digested with 0.2% collagenase (Sigma) for 60 minutes. Individual myofibers were then purified manually under a dissection microscope and either fixed immediately or maintained in suspension in growth media (DMEM, 20% FBS, 15% horse serum and 2.5 ng ml^{-1} bFGF for three days.

Time-lapse microscopy. Freshly isolated MuSC were plated at a density of 5,000 cells cm^{-2} and maintained in growth media for 35 hours prior to imaging. Cultures were then placed in a temperature and CO_2-controlled environmental chamber under an inverted microscope (Nikon TE2000E) and 10x objective lens. Images were acquired every three minutes for ten hours and analyzed using Metamorph software (Molecular Devices). Cells were immediately fixed following image acquisition.

Bioluminescence imaging. A Xenogen-100 device was used as previously described (Sacco et al., 2008). The system comprises an imaging chamber and a charge-coupled device (CCD) camera with a cryogenic refrigeration unit (Xenogen). After i.p. injection of luciferin suspended in PBS (0.1 mmol kg^{-1} body weight, Xenogen), images (60 s exposure) were acquired continuously for 15 minutes. Images were evaluated and the highest value in this sequence was used for analysis (Living Image, Xenogen).

Immunofluorescence. The antibodies used were: rabbit anti-GFP (Invitrogen), chicken anti-GFP (Abcam), rabbit anti-RFP (Rockland), mouse anti-Pax7 (DSHB), rabbit anti-Myod1 (Santa Cruz), mouse anti-Myod1 (BD Biosciences), mouse anti-myosin heavy chain (Novus Biologicals), mouse anti-embryonic myosin heavy chain (DSHB), rat anti-laminin (Millipore), rabbit anti-laminin (Sigma), rabbit anti-tenascin (Millipore), mouse anti-tenascin (Clontech), rabbit anti-fibronectin (Abcam), rabbit anti-collagen VI (Fitzgerald) and Alexa-conjugated secondary antibodies (Invitrogen). For Pax7 staining, antigen retrieval was performed and sections were post fixed with 1.5% PFA.

RNA isolation and RT-qPCR. mRNA was extracted from FACS-isolated MuSC or whole mouse muscle using the miRNeasy Micro Kit (Qiagen) and quantified with a Life Tech Qubit RNA HS Assay Kit (Life Technologies). First-strand cDNA was synthesized using the Quantitech Reverse Transcription Kit (Qiagen). RT-qPCR reactions were performed on a Stratagene MX3000P machine (Agilent Technologies) with Power SYBR Green Master Mix (Applied Biosystems), 0.25 mmol L^{-1} forward and reverse primers and cDNA derived from 0.5 ng mRNA per reaction. The following thermal cycler conditions were used: 95°C for 10 min and 50 cycles of 15 sec denaturation at 95°C, 30 sec annealing at 60°C and 30 sec extension at 72°C. Data are from 2 separate reactions performed as duplicates per condition. Relative gene expression was calculated using the $2^{-\delta\Delta CT}$ method and normalized to either Rplp0 or Gapdh expression, as indicated. For primer sequences, see Table S3.

Primer sequences for RT-PCR analyses.

Pax7	fwd	atgttcagctgggaaatccggg
	rev	tcccgaacttgattctgagcactcg
Myf5	fwd	ccaccaaccctaaccagaga
	rev	ctgttctttcgggaccagac
Myod1	fwd	ccactccgggacatagacttg
	rev	aaaagcgcaggtctggtgag
Myog	fwd	cagtgaatgcaactcccacag
	rev	atggacgtaagggagtgcaga
TnC	fwd	gagagagtgggctaaacatgac
	rev	atccactgagcattgggaac
Fn1	fwd	ggccacacctacaaccagta
	rev	tcgtctctgtcagcttgcac
Col6α1	fwd	ctgctgctacaagcctgct
	rev	ccccataaggtttcagcctca
Col6α2	fwd	aaggccccattggattccc
	rev	ctcccttccgaccatccgat
Col6α3	fwd	gctgcggaatcactttgtgc
	rev	aaggaccgtttcctgcttgtt
Hey1	fwd	tcagcgtggggaatcttaac
	rev	gattcagggcacagacacct
HeyL	fwd	gcgattgaagtccccagata
	rev	actggggtcaccagactgag
Axin2	fwd	aacctatgcccgtttcctcta
	rev	gagtgtaaagacttggtccac
Rplp0	fwd	gcaggtgtttgacaacggcag
	rev	gatgatggagtgtggcaccga
Gapdh	fwd	tgcaccaccaactgcttag
	rev	ggatgcagggatgatgttc

SUPPLEMENTAL REFERENCES

Micallef, L., and Rodgers, P. (2014). eulerAPE: drawing area-proportional 3-Venn diagrams using ellipses. PLoS ONE *9*, e101717.